Spectrum of Engineering Sciences
ISSN (e) 3007-3138 (p) 3007-312X Volume 4, Issue 2, 2026

INVESTIGATING INFLUENCE OF SLANT ANGLES ON AERODYNAMIC PERFORMANCE OF HEAVY-DUTY BUSES (HDB) THROUGH COMPUTATIONAL FLUID DYNAMICS (CFD)

Irfan Ahmed[*1], Asif Ahmed[2], Sana Imran[3], Imran Mir Chohan[4], Sanjay Kumar[5]

[1,2,4]*Faculty of Engineering Science and Technology, Department of Mechanical Engineering, Indus University, Karachi, 75850, Pakistan*
[3]*Department of Computer Science, Shah Abdul Latif University (SALU), Khairpur Mir's, Sindh, Pakistan*
[5]*Department of Fundamental and Applied Science, University Teknologi Petronas, 32610 Seri Iskandar, Perak, Malaysia*

[*1]irfanahmedph1@gmail.com

DOI: https://doi.org/10.5281/zenodo.18542319

Keywords
Heavy Duty Buses, Aerodynamics Performance, Computational Fluid Dynamic

Article History
Received: 10 December 2025
Accepted: 25 January 2026
Published: 09 February 2026

Corresponding Author: *
Irfan Ahmed

Abstract
Heavy-duty buses (HDBs) play a vital role in public transportation systems; however, their blunt body geometry results in significant aerodynamic drag, leading to high fuel consumption. Traditional experimental methods for evaluating HDB aerodynamic performance are time-consuming, resource-intensive, costly, and limit the number of design configurations that can be studied. Therefore, this study employs computational fluid dynamics (CFD) to analyse the impact of different slant angles on HDB aerodynamic performance and assesses the reliability of CFD predictions by comparing them with published experimental data. A three-dimensional bus model was created using ANSYS Design Modeller, and numerical simulations were conducted in ANSYS Fluent under appropriate boundary conditions. The rear tilt angle was systematically varied to investigate its effect on the drag coefficient. Results indicate that the rear tilt angle significantly influences aerodynamic drag, with the drag coefficient reaching its minimum at a 12.5° tilt angle. Furthermore, CFD calculations showed good agreement with experimental results, with deviations consistently below 6%. These findings validate CFD as a reliable and cost-effective tool for predicting the aerodynamic performance of heavy-duty buses.

INTRODUCTION

The heavy-duty buses (HDB) are considered a major mode of public transportation around the world [1], [2]. These buses are accessible, safe, and affordable to the large portion of the population, which also reduces traffic congestion [3], [4]. Despite their number of benefits, HDB consume significant amounts of fuel due to their bluff body and shape [5], [6]. Their geometry generates considerable aerodynamic drag, which can contribute to 10 to 20% of the total fuel usage [7]. Reducing this drag not just lowers operational costs but also provides environmental benefits [8], [9]. These benefits includes reduction on CO_2 emission during life cycle [10], [11], [12], [13]. Previously, numerous studies have been conducted on the design of the HDB to reduce the aerodynamic drag and to enhance the fuel efficiency of buses. For instance, Gilhaus [14] conducted the wind tunnel test to study the effect of cabin edges on the aerodynamic performance of HDV and found that angular-shaped cabin buses had lower aerodynamic drag than rounded cabin buses. In 2016, Aulakh [15] developed the experimental setup to investigate the influence of underbody diffuser angle on aerodynamic drag of HD-BS. His findings revealed that the underbody diffuser angle had a significant effect on the drag coefficient, and the HDB, which had a 7-degree underbody angle, had a better drag coefficient than other HDB. Additionally, Huminic et al. [16] observed similar findings while studying the impact of underbody tail angle on the aerodynamic performance of a simplified bus model. Whereas in 2016, Harun et al. [17] studied the impact of various frontal air deflectors on the aerodynamic drag of various HDVs and found that the models that were used in Pakistan had approximately a 56% higher drag reduction rate than the simplified model of air deflectors. Moreover, Ahmed et al. [18] conducted the experimental study of different HDB with various slant angles from 0 degrees to 45 degrees and found that the model that had a 12.5-degree slant angle had better aerodynamic performance than the others.

From previous literature it has been observed that the aerodynamic characteristics of buses have been assessed through wind-tunnel experiments or full-scale road tests [19], [20], [21], [22], [23]. While these experimental methods deliver accurate results, they are costly, time-intensive, and limit the number of design configurations that can be tested in the wind tunnel [24]. Therefore, in the last few decades, researchers have given attention to computational fluid dynamics (CFD) to study the aerodynamic characteristics of different systems because CFD offers a rapid, flexible, and cost-effective approach to evaluate multiple design variations without experimental resources [25]. Like in 2017, Mir et al. studied the impact of convergent angle on the aerodynamic performance of a nozzle by CFD. In their study they generated a coarse mesh of the nozzle model and found an 8% difference with experimental results. Meanwhile, in 2017, Moghimi and Rafee [26] conducted the experimental and computational study of Ahmed's 0-degree model. In their study they generated coarse mesh for computational work. Whereas their study showed 8.3% error between experimental and computational results.

Since only limited CFD-based research has been conducted on HDB, the present study aims to perform detailed CFD simulations using a refined mesh model to investigate the influence of various slant angles on aerodynamic drag. In addition, the study seeks to validate the numerical results against previously published experimental data to assess the consistency and reliability of the CFD findings.

1. Methodology

1.1. HDB Models, Meshing, and Boundary Conditions

To investigate the effect of slant angle on aerodynamic drag of HDB the simplified 0° Ahmed model have been used as a baseline model in this study as shown in Figure 1(a) [18]. The model 3D model was developed on ANSYS modeller. Additionally, different models were developed by just changing the backward slant angle from 0° to 40°. (See Figure 1(b)). The design characteristics of bus and flow filed boundary conditions are given in Table 1 and shown in Figure 2. The Reynolds number were set based on the height of model. The working medium was air. The model's ground clearance was 0.17H. The computational domain cross-sectional dimensions were set to 11H×11.7W×12.5L.

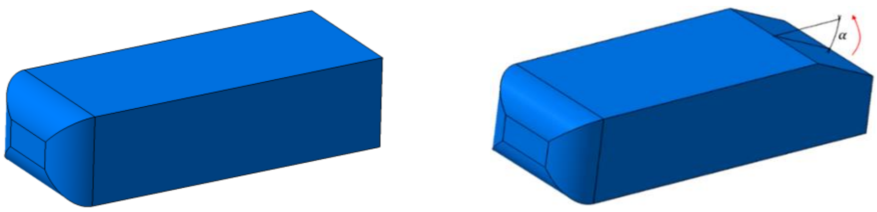

(a) 0°Ahmed model **(b)** 12.5°Ahmed model

Figure 1 Simplified models used in this study

Table 1 Design characteristics of models and initial boundary conditions

Design Parameter	Specification
Bus Length	1044mm
Width	389mm
Height	288mm
Frontal edge radius (r)	100mm
Reynolds number (Re) based on model height	1.18 × 10^6
velocity	30 m/s
Outlet Pressure	Ambient

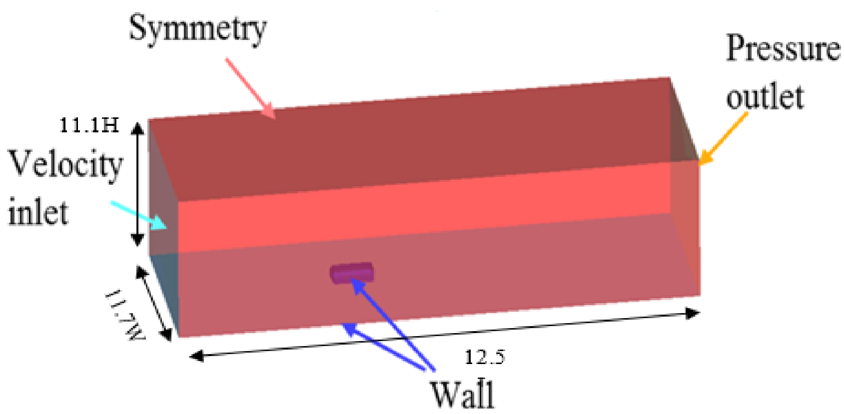

Figure 2. Computational setup of model

Furthermore, the mesh was generated using ICEM and the mesh was refined near the wall of the model. The number of meshes per vehicle was about 8-9 million. Figure 3 shows the mesh generation of the Ahmed model with a slope angle of α=12.5°. The mesh situation of other working conditions is similar. The calculation boundary conditions are: velocity inlet boundary, pressure outlet boundary, symmetrical boundary conditions on both sides and top surface, and no-slip wall boundary on bottom surface and model surface. The commercial software Fluent was used for numerical solution.

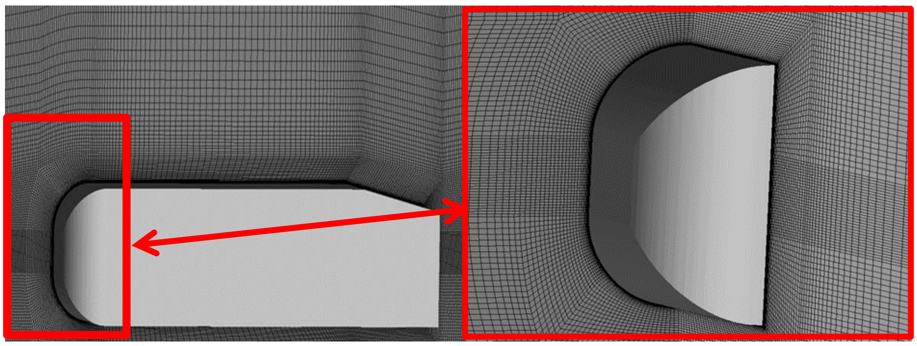

Figure 3 Mesh model for computational study

2.2. Governing Equations and Solver Settings.

The 3D steady RANS equations were solved with the two equations SST k-ω model (Menter, 1993) for closure [27]. The choice of the SST k-ω model was made based on its good effect on the simulation of the separation flow with a large adverse pressure gradient. The SST k-ω model is a combination of k-ω model appropriate for the wall region and logarithmic region of the boundary layer and k-ε model applying to the outer region of the boundary layer [28]. Compared with the standard k-ω model, the SST k-ω model weakens the influence of far-field and inlet. The governing equations of SST k-ω model are represented below

$$\rho \frac{Dk}{Dt} = \tau_{ij}\frac{\partial U_i}{\partial x_j} - \rho\beta^* k\omega + \frac{\partial}{\partial x_j}\left[\left(\mu + \frac{\mu_t}{\sigma_k}\right)\frac{\partial k}{\partial x_j}\right] \quad \text{Equation (1)}$$

Where, k, μ, μ_t, ω and τ_{ij} are turbulent kinetic energy, molecular viscous force, eddy viscosity coefficient, dissipation ratio and Reynold stress, respectively.

Furthermore, the aerodynamic drag of a body mainly comes from pressure difference drag and surface friction drag. The aerodynamic drag calculated in this paper is as follows:

$$F_x = \iint_A P dA_x + \iint_A \tau_x dA_x \quad \text{Equation (2)}$$

$$C_D = \frac{F_x}{\frac{1}{2}\rho U_\infty^2 A_x} \quad \text{Equation (3)}$$

$$\Delta C_D(\%) = 100 \times \frac{\left|C_{D\_CFD} - C_{D\_EXP}\right|}{C_{D\_EXP}} \quad \text{Equation (4)}$$

Where, P is the static pressure (relative to atmospheric pressure) on the model surface, A_x and τ_x are the windward area and frictional stress of the model along the x-direction, respectively. ρ is the air density · U_∞ is the inlet flow velocity, C_D is the drag coefficient, C_{D_CFD} and C_{D_EXP} are the numerical simulation and experimental values of the drag coefficient, respectively, and ΔC_D is the calculation error between experimental and simulation results.

2. Result and Discussion

2.1. Effects of Slant angle on drag coefficients

The aerodynamics performance of heavy-duty bus models with change of slant angles is investigated by considering the corresponding drag coefficients with the help of numerically CFD simulations based on SST k-ω model. The impacts of slant angles on drag coefficients ranging from 0° to 40° and are discussed in Figure 4 and Table 2. Simulation results reveal a non-linear relationship between slant angle and dragging coefficient. The baseline model depicts a drag coefficient of approximately 0.258 at the angle of 0°. However, a decrease in coefficient of drag was detected at the angle of 12.5°, where minimum value of 0.23 was observed. Although, a steady increment in dragging coefficient is examined beyond 15° and notable rise is observed between 20° to 30°. The findings reveal that 12.5° configuration yields an optimal aerodynamics performance. The computational results are validated with existing available experiments results [18], finding reveals a good agreement with minimum deviation below 5% for most of cases. The largest relative error (5.8%) is observed at 30° model, while least (0.84%) at 20°. This confirms that SST k-ω model and refined mesh provide reliable numerically predictions of external flow behaviors around bus-like boundaries.

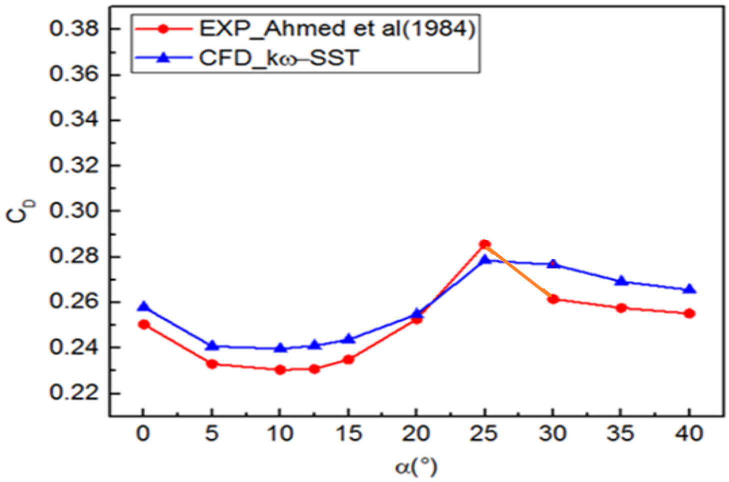

Figure 4 Effect of slant angle on Drag coefficient

Table 2 Simulation and previous experimental results

α(°)	0	5	10	12.5	15	20	25	30	35	40
C_{D_EXP}	0.250	0.233	0230	0.230	0.235	0.253	0.286	0.262	0.258	0.255
C_{D_CFD}	0.258	0.241	0.240	0.241	0.244	0.255	0.279	0.277	0.269	0.266
ΔC_D(%)	3.0%	3.3%	4.0%	4.4%	3.7%	0.84%	-2.5%	5.8%	4.5%	4.1%

Figures 5 demonstrate the velocity and streamline distributions along longitudinal symmetry plane for different slant angles. A large recirculation region is formed immediately behind the vertical surface, which leads to high dragging pressure due to low-pressure wake at the angle of α =0° as shown in Figure 5(a). Flow separation occurs sharply at roof rear junction and wake region was dominated by a large vortex structure. Whereas the slant surface promotes flow reattachment and smooth velocity transition at the optimal angle of α =12.5° as shown in Fig 5(b). The region of wake is notably decreased and pressure behind the vehicle was significantly improved. Moreover, Fig 5(c) at angle of α =25° depicts as the angle rises, the partial flow detachment occurs along the slant surface. The wake regions started to increase again, the velocity shortfall downstream becomes more pronounced. Additionally, Fig 2(d) at angle of α =35°, demonstrates flow separation take over the most of the slanted surface. Two large counter rotational vortices dominate the field of flow, which leads to an increase in drag.

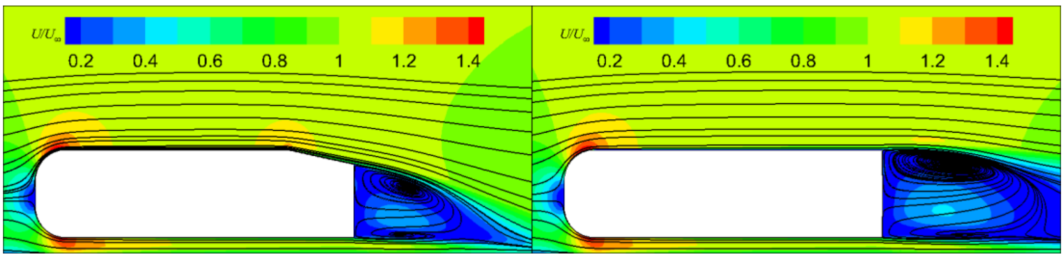

(a) α =0° **(b) α =12.5°**

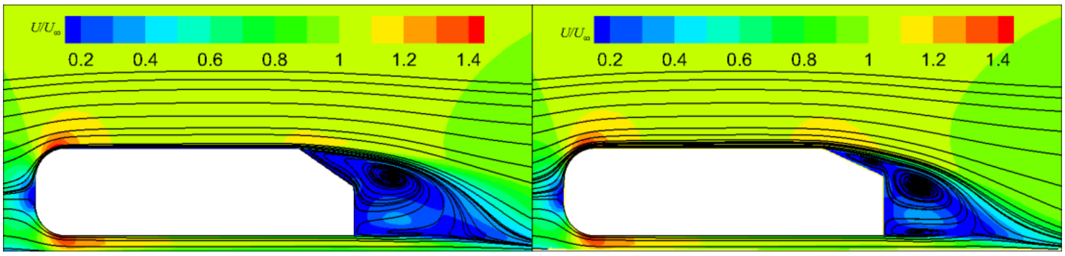

(c) α =25° **(d) α =35°**

Figure 5 Velocity and streamline distribution contours around the span wise symmetry plane

Fig 6 compares the three-dimension streamline patterns around HD-B models with several rear slant angles. This highlights the change in vortex structure, flow attachment and wake region behavior with alteration of geometry. Fig 6(a) at angle of α =0° illustrates that streamlines diverge at the rear, which causes symmetric and broad wake. Therefore, backflow intensity is high and detached flow region is wide. However, Fig 6(b) at angle of α =12.5°depicts that streamlines remain closely attached to slant surface for a longer distance before separation. Wake is narrow, with more stable and ordered vortex shedding. This optimal result has shown improved aerodynamic stability and reduction in pressure drag. Whereas Fig 6(c) at angle of α =35° depicts streamlines detach prematurely, unstable vortex pairs and large scale that oscillate in the near wake region. Therefore, enlarged separation bubble and turbulent mix zone resulted in high total drag and unsteady aerodynamic behavior. The 12.5° configuration achieves optimal balance between surface pressure and wake stability, whereas excessive inclination (≥ 35°) results to dominate vortex formation and significant aerodynamic losses.

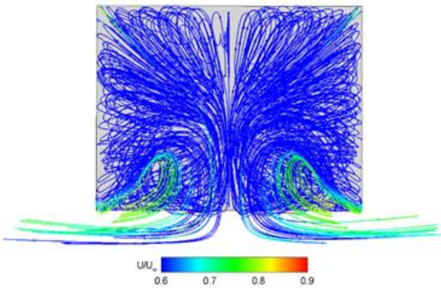

(a) **α**=0°

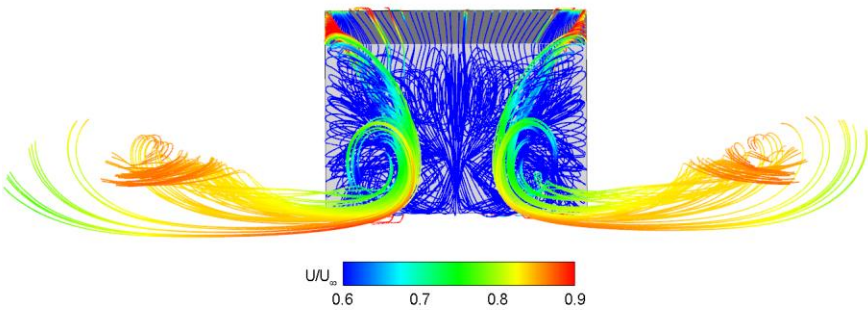

(b) **α**=12.5°

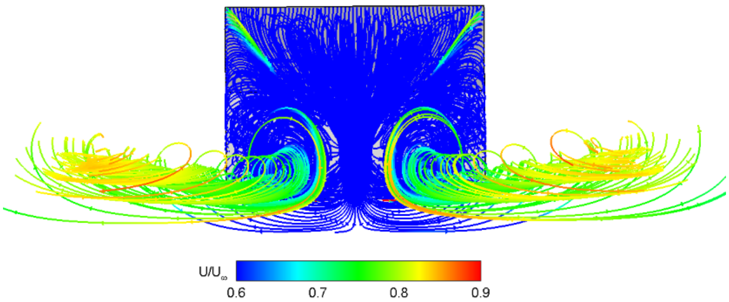

(c) α=35°

Figure 6 Backside streamline distribution of models with different slant angles.

3. Conclusion

In this study the CFD simulation was conducted to study the aerodynamics performance of HDB with respect to different slant angles. From finding of this research following conclusions are drawn.

- The slant angle had significant effect on aerodynamics drag of HDB, where the optimal drag coefficient was around 0.230 with the model having slant angle 12.5°.
- All CFD results showed close alignment with previous experimental results and the error remained between 0.8% to 5.8%.
- CFD is the efficient method that can assess the aerodynamic performance of HDB without experimental resources.
- CFD has capability of in-depth visualisation of flow behaviour around HDB.

References

[1] O. Siddiqui, H. Ishaq, D. A. Khan, and H. Fazel, “Social cost-benefit analysis of different types of buses for sustainable public transportation,” *J. Clean. Prod.*, vol. 438, 2024, doi: 10.1016/j.jclepro.2024.140656.

[2] Muhamad Nazri Borhan, Ahmad Nazrul Hakimi Ibrahim, Deprizon Syamsunur, and Riza Atiq Rahmat, “Why Public Bus is a Less Attractive Mode of Transport: A Case Study of Putrajaya, Malaysia,” *Period. Polytech. Transp. Eng.*, vol. 47, no. 1, pp. 82–90, 2019, [Online]. Available: file:///C:/Users/lenovo/Downloads/9228-Article Text PDF-30469-3-10-20181214.pdf

[3] M. Hadid, M. Z. Irawan, D. Parikesit, F. Firzan, N. H. Yunianti, and N. O. Widiastuti, “Driving the future of sustainable public transport: a literature review on challenges and strategies in the adoption of autonomous buses,” *Discov. Sustain.*, vol. 6, no. 1, 2025, doi: 10.1007/s43621-025-01112-0.

[4] E. Sogbe, S. Susilawati, and T. C. Pin, “Scaling up public transport usage: a systematic literature review of service quality, satisfaction and attitude towards bus transport systems in developing countries,” *Public Transp.*, vol. 17, no. 1, pp. 1–44, 2025, doi: 10.1007/s12469-024-00367-6.

[5] M. C. Rozina Chohan, Imran Mir Chohan, “Comparative Analysis of Different Convergent Dection Angles and Working Fluids on Supersonic Nozzle Thrust Force by Computational Fluid Dynamic (CFD),” *Tech. J.*, vol. Vol 30, no. 02, 2025.

[6] I. MIR, S. SAMO, T. HUSSAIN, I. ALI, and H. A. K. DURANI, “Influence of Convergent Section Length and Angle on Performance of Supersonic Nozzle,” *Sindh Univ. Res. J. -Science Ser.*, vol. 49, no. 004, pp. 727--732, 2017, doi: 10.26692/surj/2017.12.48.

[7] M. R. Rony, M. J. Islam, S. Shahriare, and M. M. Alam, "Optimizing Fuel Efficiency in Intercity Buses: Aerodynamic Design Enhancements and Implications for Sustainable Transportation in Bangladesh," *J. Appl. Fluid Mech.*, vol. 17, no. 12, pp. 2592–2607, 2024, doi: 10.47176/jafm.17.12.2664.

[8] M. Ehsani, A. Ahmadi, and D. Fadai, "Modeling of vehicle fuel consumption and carbon dioxide emission in road transport," *Renew. Sustain. Energy Rev.*, vol. 53, pp. 1638–1648, 2016, doi: 10.1016/j.rser.2015.08.062.

[9] Afsheen, Mujtaba Hassan, Imran Mir Chohan, Sadaquat Hussain, and Raja Zafar Ali, "Supply Chain Management Impact on Project Performance in Construction," *Spectr. Eng. Sci.*, vol. 3, no. 8, 2025, [Online]. Available: https://doi.org/10.5281/zenodo.16886237

[10] M. Ali, "Valorization of sewage sludge ash in alkali-activated materials: A comprehensive review of material properties, reactivity, and future sustainable applications," *Chemosphere*, vol. 391, 2025, doi: 10.1016/j.chemosphere.2025.144724.

[11] I. M. Chohan, A. Ahmad, N. Bheel, T. Najeh, and A. H. Almaliki, "Sustainability assessment of different pipeline materials in freshwater supply systems," *Front. Mater.*, vol. 12, 2025, doi: 10.3389/fmats.2025.1566151.

[12] N. Bheel *et al.*, "Optimization of durability characteristics of engineered cementitious composites combined with titanium dioxide as a nanomaterial applying RSM modelling," *Sci. Rep.*, vol. 15, no. 1, 2025, doi: 10.1038/s41598-025-94382-7.

[13] I. M. Chohan, A. Ahmad, N. Sallih, N. Bheel, M. Ali, and A. F. Deifalla, "A review on life cycle assessment of different pipeline materials," *Results Eng.*, vol. 19, 2023, doi: 10.1016/j.rineng.2023.101325.

[14] A. Gilhaus, "The influence of cab shape on air drag of trucks," *J. Wind Eng. Ind. Aerodyn.*, vol. 9, no. 1–2, pp. 77–87, 1981, doi: 10.1016/0167-6105(81)90079-9.

[15] D. J. S. Aulakh, "Effect of Underbody Diffuser on the Aerodynamic Drag of Vehicles in Convoy," *Int. J. Veh. Struct. Syst.*, vol. 9, no. 3, pp. 164–168, 2017, doi: 10.4273/ijvss.9.3.06.

[16] A. Huminic, G. Huminic, and A. Soica, "Study of aerodynamics for a simplified car model with the underbody shaped as a Venturi nozzle," *Int. J. Veh. Des.*, vol. 58, no. 1, pp. 15–32, 2012, doi: 10.1504/IJVD.2012.045927.

[17] H. Chowdhury, B. Loganathan, I. Mustary, H. Moria, and F. Alam, "Effect of Various Deflectors on Drag Reduction for Trucks," *Energy Procedia*, vol. 110, pp. 561–566, 2017, doi: 10.1016/j.egypro.2017.03.185.

[18] S. R. Ahmed, G. Ramm, and G. Faltin, "Some salient features of the time-averaged ground vehicle wake," *SAE Tech. Pap.*, 1984, doi: 10.4271/840300.

[19] X. He *et al.*, "Wind tunnel tests on the aerodynamic characteristics of vehicles on highway bridges," *Adv. Struct. Eng.*, vol. 23, no. 13, pp. 2882–2897, 2020, doi: 10.1177/1369433220924791.

[20] R. Wood, "A Review of Reynolds Number Effects on the Aerodynamics of Commercial Ground Vehicles," *SAE Int. J. Commer. Veh.*, vol. 5, no. 2, pp. 628–639, 2012, doi: 10.4271/2012-01-2045.

[21] I. M. Chohan, A. Ahmad, N. Sallih, N. Bheel, and A. Almaliki, "Correction: Effect of seawater salinity and temperature on material performance and marine ecotoxicity of offshore pipeline using RSM modelling," *Int. J. Environ. Sci. Technol.*, vol. 23, no. 3, 2026, doi: 10.1007/s13762-025-07011-1.

[22] I. M. Chohan, A. Ahmad, N. Sallih, N. Bheel, and A. H. Almaliki, "Effect of seawater salinity and temperature on material performance and marine ecotoxicity of offshore pipeline using RSM modelling," *Int. J. Environ. Sci. Technol.*, vol. 23, no. 2, 2026, doi: 10.1007/s13762-025-06869-5.

[23] I. Mir Chohan *et al.*, "Corrosion Behaviour and Microhardness of ASTM 106 Grade B Carbon Steel Offshore Pipeline at Different Locations in Malaysia," *J. Adv. Res. Micro Nano Eng. J. homepage*, vol. 38, pp. 1–11, 2025, [Online]. Available: https://semarakilmu.com.my/journals/index.php/micro_nano_engineering/index

[24] D. H. Aseba, R. B. Nallamothu, and A. Kahsay, "Numerical and Experimental Analysis of Base Cavity and Windshield Angle for Aerodynamic Drag Reduction of a Bus," *J. Eng. (United Kingdom)*, vol. 2025, no. 1, 2025, doi: 10.1155/je/7894397.

[25] J. B. Kodman, B. Singh, and M. Murugaiah, "A Comprehensive Survey of Open-Source Tools for Computational Fluid Dynamics Analyses," *J. Adv. Res. Fluid Mech. Therm. Sci.*, vol. 119, no. 2, pp. 123–148, 2024, doi: 10.37934/arfmts.119.2.123148.

[26] P. Moghimi and R. Rafee, "Numerical and Experimental Investigations on Aerodynamic Behavior of the Ahmed Body Model with Different Diffuser Angles ," *J. Appl. Fluid Mech.*, vol. 11, no. 4, pp. 1101–1113, 2018.

[27] Y. Egorov and F. Menter, "Development and application of SST-SAS turbulence model in the DESIDER project," *Notes Numer. Fluid Mech. Multidiscip. Des.*, vol. 97, pp. 261–270, 2008, doi: 10.1007/978-3-540-77815-8_27.

[28] S. Kumar, H. Sakidin, M. Zafar, H. B. Lanjwani, and I. M. Chohan, "Nanofluid Thermophysical Property Modelling for Enhanced Oil Recovery: A Comprehensive Review and Future Outlook for Artificial Intelligence Integration," *Arch. Comput. Methods Eng.*, 2025, doi: 10.1007/s11831-025-10329-1.